Camalexin is synthesized from indole-3-acetaldoxime, a key branching point between primary and secondary metabolism in *Arabidopsis*

Erich Glawischnig*†‡, Bjarne Gram Hansen*, Carl Erik Olsen*, and Barbara Ann Halkier*

*Center for Molecular Plant Physiology and Department of Plant Biology, Royal Veterinary and Agricultural University, Thorvaldsensvej 40, DK-1871 Frederiksberg C, Copenhagen, Denmark; and †Institute for Genetics, Technical University Munich, Am Hochanger 8, D-85350 Freising, Germany

Edited by Rodney B. Croteau, Washington State University, Pullman, WA, and approved April 7, 2004 (received for review September 12, 2003)

Characteristic for cruciferous plants is their production of N- and S-containing indole phytoalexins with disease resistance and cancer-preventive properties, previously proposed to be synthesized from indole independently of tryptophan. We show that camalexin, the indole phytoalexin of *Arabidopsis thaliana*, is synthesized from tryptophan via indole-3-acetaldoxime (IAOx) in a reaction catalyzed by CYP79B2 and CYP79B3. *Cyp79B2*/*cyp79B3* double knockout mutant is devoid of camalexin, as it is also devoid of indole glucosinolates [Zhao, Y., Hull, A. K., Gupta, N. R., Goss, K. A., Alonso, J., Ecker, J. R., Normanly, J., Chory, J. & Celenza, J. L. (2002) *Genes Dev.* 16, 3100–3112], and isotope-labeled IAOx is incorporated into camalexin. These results demonstrate that only CYP79B2 and CYP79B3 contribute significantly to the IAOx pool from which camalexin and indole glucosinolates are synthesized. Furthermore, production of camalexin in the *sur1* mutant devoid of glucosinolates excludes the possibility that camalexin is derived from indole glucosinolates. CYP79B2 plays an important role in camalexin biosynthesis in that the transcript level of *CYP79B2*, but not *CYP79B3*, is increased upon induction of camalexin by silver nitrate as evidenced by microarray analysis and promoter–β-glucuronidase data. The structural similarity between cruciferous indole phytoalexins suggests that these compounds are biogenetically related and synthesized from tryptophan via IAOx by CYP79B homologues. The data show that IAOx is a key branching point between several secondary metabolic pathways as well as primary metabolism, where IAOx has been shown to play a critical role in IAA homeostasis.

Characteristic for cruciferous plants is the synthesis of a wide range of species-specific phytoalexins that structurally are sulfur-containing indole alkaloids (1) and the synthesis of glucosinolates (reviewed in ref. 2). Both groups of natural products are involved in plant defense and have cancer-preventive properties (3, 4). Very little is known about the biosynthetic pathway of the S-containing indole phytoalexins. Their similar structure with N- and S-containing side chains at C-3 of the indole ring suggests a biogenetic relationship (5). Camalexin (3-thiazol-2′-yl-indole) is produced in the model plant *Arabidopsis thaliana* (6). It is induced by a variety of microorganisms, e.g., *Pseudomonas syringae* (6) and *Alternaria brassisicola* (7), and by abiotic factors, such as $AgNO_3$ (8). These findings make camalexin a good model compound for studying biosynthesis and regulation of cruciferous indole phytoalexins. *In vivo* feeding experiments where radiolabeled anthranilate and tryptophan were applied on leaves treated with $AgNO_3$ led to the suggestion that tryptophan was not a precursor in camalexin biosynthesis because tryptophan was much less efficiently incorporated into camalexin compared with anthranilate (8, 9). The data were further supported by labeling studies performed in three tryptophan mutants (8), where reduced levels of camalexin accumulated in *trp1–100* with an impaired anthranilate transferase but not in *trp3–1* and *trp2–1* mutants with mutations in the α and β subunits of tryptophan synthase, respectively. *In vivo* feeding experiments with radiolabeled anthranilate and indole showed that indole was most efficiently incorporated into camalexin, and that feeding of anthranilate was followed by a transient accumulation of indole (10). Accordingly, it was suggested that indole destined for camalexin is produced by a pathway that does not involve tryptophan synthase (10) but, e.g., a homolog of the α-subunit tryptophan synthase such as BX1 from maize that catalyzes the formation of indole in 2,4-dihydroxy-7-methoxy-1,4-benzoxazin-3-one biosynthesis (11).

Glucosinolates are derived from amino acids that are converted to the corresponding oximes by cytochromes P450 belonging to the CYP79 family (2). In *Arabidopsis*, CYP79B2 (12, 13) and CYP79B3 (12) catalyze the conversion of tryptophan into indole-3-acetaldoxime (IAOx) that is channeled by the oxime-metabolizing CYP83B1 into the biosynthetic pathway of indole glucosinolates (14, 15). Furthermore, IAOx has been shown to be a precursor of the phytohormone indole-3-acetic acid (IAA) as evidenced by enzyme studies with radiolabeled IAOx (16) and the high-auxin phenotype of knockout mutants in postoxime enzymes in glucosinolate biosynthesis, such as *sur1* (17) and *sur2* (14, 18). Based on structural similarity, it has been suggested that brassinin and possibly other cruciferous phytoalexins were derived from the indole glucosinolate glucobrassicin (5). However, in a recent *in vivo* feeding study in turnip (*Brassica rapa*) roots with deuterated IAOx and glucobrassicin, IAOx, and not glucobrassicin, was incorporated into brassinin and brassinin-derived phytoalexins, indicating that IAOx is an intermediate in brassinin biosynthesis (19).

In this manuscript, we show that camalexin is synthesized from tryptophan via IAOx by CYP79 homologues, and that it is not derived from indole glucosinolates. Furthermore, we provide data that indicate that CYP79B2 and CYP79B3 have differential functions in camalexin biosynthesis.

Methods

Plant Material. *Cyp79B2*, *cyp79B3*, and *cyp79B2/cyp79B3* knockout mutants (20) originating from the Salk Institute collection were kindly provided by Y. Zhao (University of California at San Diego, La Jolla). Generation of *35S::CYP79B2* has been described (13). Seeds of *sur1–3* were a kind gift from C. Bellini (Institut de la Recherche Agronomique, Versailles, France). All mutants and transgenic lines are in Col-0 background. Plants were grown in soil mixed with sand (3:1) in a walk-in growth chamber (HEMZ 20/240/S, Heraeus) at 12 h light, 80–100 μmol of photons per m^2 per sec, 18°C, and 40% relative humidity.

Silver Nitrate Induction and Extraction of Camalexin. For camalexin induction, 4- and 6-week-old rosette leaves were sprayed with a thin

This paper was submitted directly (Track II) to the PNAS office.

Abbreviations: 6-F-IAOx, 6-fluoro-indole-3-acetaldoxime; GUS, β-glucuronidase; IAA, indole-3-acetic acid; IAOx, indole-3-acetaldoxime.

‡To whom correspondence should be addressed. E-mail: egl@wzw.tum.de.

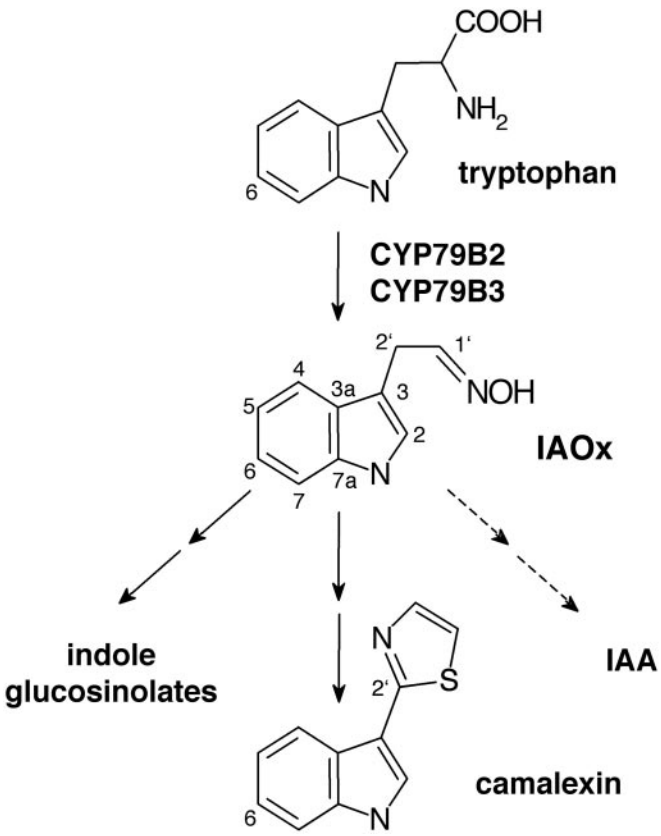

Fig. 1. Schematic view of biosynthetic pathways of IAOx-derived indole compounds in *Arabidopsis*.

film of 5 mM $AgNO_3$/0.02% Silwet L-77. Until harvest, plants were covered with a transparent plastic hood to avoid desiccation. For each measurement, three leaves were cut at the petiole, weighed, and frozen in liquid nitrogen. Camalexin was extracted as described (6), with the following minor modifications. Extraction was performed twice for 30 min in 600 μl of MeOH/H_2O (1:1) at 60°C. Samples were analyzed by reverse-phase HPLC (LiChroCART 250-4, RP-18, 5 μm, Merck; 1 ml·min^{-1} MeOH/H_2O (3:2) for 1 min, followed by a 14-min linear gradient to 100% MeOH and then 3 min at 100% MeOH). The peak at 16.2 min was identified as camalexin by comparison with authentic standard with respect to retention time and UV spectrum (photodiode array detector 168, Beckman Instruments, Fullerton, CA) and quantified by using a Shimadzu F-10AXL fluorescence detector (318 nm excitation and 370 nm emission) and by UV absorption at 318 nm.

Synthesis of Labeled IAOx. IAOx was synthesized chemically from indole-3-acetaldehyde, [2′-^{14}C]IAOx was synthesized from [3′-^{14}C]tryptophan, and 6-fluoro-indole-3-acetaldoxime (6-F-IAOx) was synthesized from 20 mg 6-F-tryptophan, essentially as described (21). R_f values of 0.35 and 0.21 were determined for 6-F-indole-3-acetaldehyde and 6-F-IAOx, respectively, in TLC analysis ($CHCl_3$/MeOH, 96:4). IAOx and 6-F-IAOx were characterized by NMR (Avance 400, Bruker, Billerica, MA, in MeOH-*d4*, ^{1}H at 400.1 and ^{13}C at 100.6 Mhz). δ_H values are relative to internal TMS and δ_C-values are based on δ_C(MeOH-*d4*) = 49.05. Assignments (Fig. 1) are based on 1D spectra (^{1}H, ^{13}C, and distortionless enhancement by polarization transfer) as well as 2D spectra (COSY, heteronuclear sequential quantum correlation, heteronuclear multiple bond correlation, and *J*-resolved 2D correlation). Some chemical shifts have been retrieved from the 2D spectra. The (*E*)- and (*Z*)-isomers were present in a ratio of ≈2:1 and ≈17:1 for IAOx and 6-F-IAOx, respectively.

(*E*)-IAOx. ^{1}H NMR: 7.10 (br s, H-2), 7.507 (dt, J = 7.9/1.0, H-4), 6.997 (m, J = 7.5 1.1, H-5), 7.094 (m, J = 7.6 1.2, H-6), 7.336 (dt, J = 8.2/1.0, H-7), 6.79 (t, $J_{1',2'}$ = 5.3, H-1′), 3.80 (dd, J = 5.3/0.9, H-2′). ^{13}C NMR: 123.7 (C-2), 111.1 (C-3), 119.2 (C-4), 119.8 (C-5), 122.6 (C-6), 112.3 (C-7), 128.7 (C-3a), 138.3 (C-7a), 152.1 (C-1′), 22.3 (C-2′).

(*Z*)-IAOx. ^{1}H NMR: 7.07 (br s, H-2), 7.54 (dt, J = 8.0/1.0, H-4), 6.994 (m, J = 7.5 1.2, H-5), 7.33 (dt, J = 8.2/0.9, H-7), 7.48 (t, J = 6.4, H-1′), 3.60 (dd, J = 6.4/0.9, H-2′). ^{13}C NMR: 123.7 (C-2), 119.4 (C-4), 128.7 (C-3a), 151.4 (C-1′), 26.9 (C-2′).

(*E*)-6-F-IAOx. ^{1}H NMR: 7.10 (t, J = 0.9, H-2), 7.46 (dd, $J_{4,5}$ = 8.7 $J_{4,F}$ = 5.3, H-4), 6.79 (ddd, $J_{4,5}$ = 8.7, $J_{5,7}$ = 2.3, $J_{5,F}$ = 9.8, H-5), 7.03 (br dd, $J_{5,7}$ = 2.3, $J_{7,F}$ = 10.0, H-7), 6.77 (t, $J_{1',2'}$ = 5.4, H-1′), 3.78 (dd, $J_{1',2'}$ = 5.4, $J_{2,2'}$ = 0.9, H-2′). ^{13}C NMR: C-2: 124.2 (C-2), 111.4 (C-3), 120.2 ($J_{C,F}$ = 10, C-4), 108.2 ($J_{C,F}$ = 25, C-5), 161.3 ($J_{C,F}$≈220, C-6), 98.2 ($J_{C,F}$ = 26, C-7), 125.5 (C-3a), 138.2 (C-7a), 151.7 (C-1′), 22.2 (C-2′).

(*Z*)-6-F-IAOx. ^{1}H NMR: 7.06 (t, $J_{2,10}$ = 0.9, H-2), 7.47 (H-1′), 3.58 (dd, $J_{1',2'}$ = 6.4, $J_{2,2'}$ = 0.9, C-2′). ^{13}C NMR: 124.8 (C-2), 151.2 (C-1′), 27.0 (C-2′).

***In Vivo* Labeling Experiments.** For each sample, fluoro- or ^{14}C-labeled tracers of indole, tryptophan, and IAOx were incubated with three 6-week-old *Arabidopsis* rosette leaves for 16 h, starting 8 h after treatment with 5 mM $AgNO_3$. For fluorolabeling, leaves were cut at their petiole and incubated in 150 μl of 0.5 mM fluorinated precursor with or without 0.5 or 2.5 mM unlabeled competitor in H_2O/EtOH/DMSO (96.5/0.5/3). Extracts were analyzed on an Agilent (Santa Clara, CA) 1100 LC liquid chromatograph-MS coupled to a Bruker Esquire 3000Plus ion trap spectrometer (electrospray ionization in positive mode). A 2-mm ID XTerra C_{18} column (Waters) was used (0.2 ml/min, solvent A, H_2O with 0.1% formic acid; solvent B, 80% acetonitrile with 0.1% formic acid; 0–2 min 10% B, 2–10 min 10–100% B, 10–20 min 100% B). Camalexin (R_t = 13.8 min) and 6-F-camalexin (R_t = 14.6 min) were quantified from the selected ion trace chromatogram of m/z 201 and m/z 219, respectively.

To confirm their identity, camalexin and 6-F-camalexin were purified by HPLC from an extract of 30 leaves labeled with F-IAOx, as described above, and analyzed by GC-MS with a HP5890 Series II gas chromatograph (Hewlett–Packard) coupled to a JEOL JMS-AX505W mass spectrometer (source conditions: electrospray ionization mode and 70 eV at 200°C) with head pressure at 100 kPa and splitless injection. An SGE column (BPX5, 25 m × 0.25 mm, 0.22-mm film thickness) was used. The oven temperature program was 80°C for 2 min, 80–200°C at 20°C/min, 200–300°C at 5°C/min, and 300°C for 30 min. The molecular ion was base peak for camalexin as well as 6-F-camalexin (at m/z 200 and 218), and R_t was 17.6 and 17.4 min, respectively.

For ^{14}C-precursors, the labeling method was modified to avoid a strong unknown background signal comigrating with camalexin in the TLC analysis after feeding with [2′-^{14}C]IAOx. The cuticula was removed with a razor blade, and 10 μl (1 nCi/μl; 1 Ci = 37 GBq) of indole (50 mCi/mmol), tryptophan (58.1 mCi/mmol), and IAOx (58.1 mCi/mmol), respectively, in H_2O/EtOH (1:1) was spotted on each leaf in 1-μl droplets. After 16 h, extracts of the leaves were separated by TLC ($CHCl_3$/MeOH, 9:1) and analyzed on a Storm 860 phosphorimager (Amersham Pharmacia). Radiolabeled bands comigrating with camalexin were analyzed. Background from parallel analysis of extracts of noninduced plants was subtracted.

RNA Isolation and Microarray Analysis. The custom-designed oligoarray used in this experiment contains oligonucleotide probes (50-mers) for 244 cytochromes P450, 107 glycosyltransferases, 35 genes from aromatic amino acid biosynthesis, 53 genes from secondary metabolism, 9 normalization genes, and 6 control genes. Probes were printed in duplicate, i.e., each gene was represented twice on each array. Each of the genes had been manually annotated (C. Kristensen and S. Bak, personal communication), and this information was used by MWG Biotec (Ebersberg, Germany) to design gene-specific 50-mer oligonucleotides (22). Synthesis of oligonucleotides and microarray fabrication was performed by MWG Biotec. Six-week-old plants were sprayed with 5 mM $AgNO_3$/0.02% Silwet L-77 or 0.02% Silwet L-77 (control) and incubated for 16 h. Total RNA was isolated from eight leaves by using TRIzol reagent (Life Technologies, Rockville, MD). Twenty micrograms of each RNA sample (one control and one treated sample) was reverse transcribed, labeled with Cy3 and Cy5, and purified by using the RPN 5660 Cy Scribe cDNA Post Labeling Kit and the GFX purification kit (Amersham Pharmacia). Sample tubes containing Cy3- and Cy5-labeled cDNA were pooled and dried under vacuum to a final volume of 1 μl, and 15 μl of formamide hybridization buffer (MWG Biotec) was added. Before hybridization, the probe was left at 95°C for 2 min and then applied to the microarray under a coverslip. Slides were placed in hybridization chamber, and 10 μl of H_2O was placed in each corner of the chamber before sealing. Slides were incubated for 15 h at 42°C, followed sequentially by washes for 5 min in 2× SSC (1× SSC = 0.15 M sodium chloride/0.015 M sodium citrate, pH 7)/0.1% SDS, 0.5× SSC/0.1% SDS, and finally in 0.5× SSC. Slides were dried by centrifugation at 3,000 × *g* for 5 min.

Microarrays were scanned with a GMS 418 Array Scanner (Genetic MicroSystems, Woburn, MA). The two channels were normalized with respect to signal intensity by adjusting photomultiplier and laser power settings such that the number of saturated spots was the same in the two channels. The microarray analysis, image analysis, and signal quantification were performed by using IMAGENE 5.5 and GENESIGHT 3.5.2 (Biodiscovery, San Francisco). Background correction was performed, and spots showing a signal value lower than twice the background value were discarded. The experiment was performed twice, which result in four ratio values for each gene because one slide contains two replicate spots. Statistically significantly expressed genes were obtained by using SAM statistical software (23).

Generation of *CYP79B3p*::β-*glucuronidase* (*GUS*) Plants and Infection with *P. syringae*. A 2,668-bp fragment, containing 2,413 bp of the promoter and 255 bp of the 5′ end of the coding region of *CYP79B3*, was PCR amplified from gDNA of *Arabidopsis* (Col-0) by using the primers 5′-tagtcagatctaccatgggtcctggcgggagaggatg-3′ introducing a *Bgl*II restriction site at the 3′ end and 5′-gctacactgcaggtccattagtattagtttgaggttggag-3′ introducing a *Pst*I restriction site at the 5′ end. The fragment was digested with *Pst*I and *Bgl*II and ligated into pCambia 3301. *Arabidopsis* (Col-0) transformants were selected with Basta. Generation of *CYP79B2p*::*GUS* plants and GUS staining has been described (13). Infection with *P. syringae* was performed at 24°C (24) by using a suspension of the strain DC3000/*avrRps4* (25) at OD_{600} 0.1 in 10 mM $MgCl_2$.

Results

IAOx Is a Precursor of Camalexin. The role of IAOx as intermediate in camalexin biosynthesis was investigated by *in vivo* feeding of isotope-labeled indole, tryptophan, and IAOx to *Arabidopsis* leaves in which camalexin production was induced by spraying with $AgNO_3$ (8). We used this treatment because it is highly reproducible and eliminates the contribution of microbial metabolic activity. Spraying with 0.02% Silwet L-77 alone did not result in camalexin formation (data not shown). When $AgNO_3$-treated leaves were incubated with 6-F-indole, 6-F-tryptophan, and 6-F-IAOx all three compounds were shown to be precursors for 6-F-camalexin because 27 ± 2% (n = 2), 12 ± 1% (n = 2), and 60 ± 2% (n = 2), respectively, of total camalexin was fluorinated as calculated after liquid chromatography-MS analysis. Addition of an equal amount or a 5-fold molar excess of unlabeled IAOx in combination with 0.5 mM 6-F-IAOx yielded, respectively, 31% and 14% fluorinated camalexin, suggesting that 6-F-IAOx incorporation is not due to discrimination between hydrogen and fluoro substitution. Similarly, administration of ^{14}C-labeled indole, tryptophan, and IAOx resulted in incorporation into camalexin of, respectively, 20 ± 7.0, 3.5 ± 1.2, and 8.9 ± 4.6 nCi/μg camalexin (n = 4).

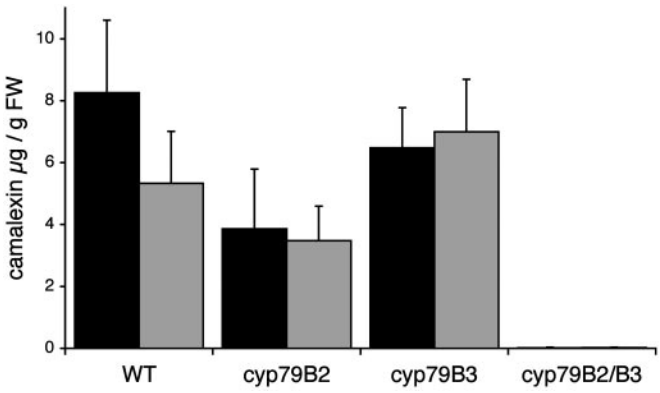

Fig. 2. Induction of camalexin in leaves of *Arabidopsis* after treatment with $AgNO_3$. Camalexin was measured in plant extracts from WT, *cyp79B2*, *cyp79B3*, and *cyp79B2*/*cyp79B3* mutants 24 h after treatment with 5 mM $AgNO_3$. Black bars are 4-week-old plants (n = 6), and gray bars are 6-week-old plants (n = 10).

Camalexin Levels in *cyp79B2*/*cyp79B3* and Other Knockout Mutants. We analyzed the production of camalexin in rosette leaves of 4- and 6-week-old plants of single knockout mutants of *cyp79B2* and *cyp79B3*, and in *cyp79B2*/*cyp79B3* double mutants (20), to investigate the origin of the IAOx involved in camalexin biosynthesis (Fig. 2). A sensitive HPLC method based on fluorescence for quantification of camalexin was used allowing detection of 1 pmol of camalexin. Twenty-four hours after $AgNO_3$ treatment, 4- and 6-week-old WT plants synthesized, respectively, 8.3 ± 2.3 and 5.3 ± 1.7 μg of camalexin per g of fresh weight, whereas less than 1% of the WT level (18 ± 16 and 19 ± 15 ng/g, respectively) was detected in the *cyp79B2*/*cyp79B3* double mutant. In the *cyp79B2* single mutant, a tendency toward reduced camalexin production was observed in comparison with WT and *cyp79B3* mutant (Fig. 2). Six-week-old *35S*::*CYP79B2* plants synthesized WT levels of camalexin (5.6 ± 2.1 μg/g, n = 6).

We investigated camalexin concentrations in the "high-auxin" mutant *sur1* that is completely devoid of glucosinolates (17). Four-week-old *sur1* mutants grown on Murashige and Skoog medium synthesized 2.1 ± 0.7 μg of camalexin per g (n = 5). This finding demonstrates that camalexin is not derived from indole glucosinolates or its degradation products. To test whether the reduced camalexin production in *sur1* was an effect of high auxin levels, WT seedlings were grown for 4 weeks on Murashige and Skoog medium containing 1 μM of the auxin 2,4-D. This treatment yielded a decrease in camalexin production (0.34 ± 0.05 μg/g, n = 4) compared with 3.6 ± 2.7 μg/g (n = 7) in seedlings grown on Murashige and Skoog medium without 2,4-D. This finding suggests that the high level of auxin in *sur1* is inhibitory to camalexin production.

Camalexin levels in 6-week-old *pad3* (*phytoalexin deficient* 3)

Table 1. Microarray data of genes significantly induced in *Arabidopsis* rosette leaves 16 h after spraying with $AgNO_3$

Gene	Locus	Up-regulation, fold
AAD23027	At2g24850	15.9
CYP82G1	At3g25180	10.7
CYP71A18	At1g11610	4.5
CYP71A12	At2g30750	3.5
AAC31939	At5g54140	3.4
CYP79B2	At4g39950	3.0
CAB88998	At3g44300	2.8
CAA73905	At1g51760	2.5
CAA23026	At4g23600	2.4
CAB89000	At3g44320	2.0

Four independent experiments were performed on an custom-designed oligoarray representing all *Arabidopsis* cytochromes P450 (CYP) and selected metabolic genes (see *Methods*).

plants (26) that are mutated in *CYP71B15*, which is suggested to be involved in camalexin biosynthesis, was ≈2% of WT level (0.13 ± 0.11 μg/g, $n = 6$), as previously shown (27). The presence of camalexin in induced *cyp71B15/pad3* plants was confirmed by liquid chromatography-MS.

Induction of *CYP79B2*. Analysis of gene expression following treatment with $AgNO_3$ was performed by probing a custom-designed oligoarray, which carries a selection of *Arabidopsis* genes including all cytochromes P450, with labeled RNA isolated 16 h after $AgNO_3$ treatment, at which time point camalexin is synthesized at a high rate (8). Twenty-five genes were significantly (>2-fold) induced or repressed (Tables 1 and 2). Specifically, *CYP79B2* was induced 3-fold, whereas no significant up-regulation of *CYP79B3* was observed (Table 1). *CYP71B15/PAD3*, suggested to be involved in camalexin biosynthesis (26), was not up-regulated.

Tissue-specific induction of *CYP79B2* was further investigated in 6-week-old *CYP79B2p*::*GUS* plants (13). As shown above, basal levels of *CYP79B2* were expressed in untreated rosette leaves (Fig. 3*A*). After $AgNO_3$ treatment, enhanced GUS expression was observed in tissue surrounding cells showing symptoms of hypersensitive response (Fig. 3 *B* and *C*). After infiltration of the plants with *P. syringae* DC3000/*avrRps4*, strong GUS staining was observed (Fig. 3 *D* and *E*), whereas control leaves infiltrated with 10 mM $MgCl_2$ showed a weak, wounding-induced response (Fig. 3*F*). In comparison, *CYP79B3p*::*GUS* plants showed higher constitutive GUS expression (Fig. 3*G*), but no enhanced GUS expression was detected after $AgNO_3$ treatment (Fig. 3*H*). *CYP79B3* expression in plants infiltrated with *P. syringae* (Fig. 3*I*) was comparable with *CYP79B3* expression in plants infiltrated with 10 mM $MgCl_2$ (Fig. 3*J*), indicating that the observed expression reflects a wounding-induced response.

Table 2. Microarray data of genes significantly repressed in *Arabidopsis* rosette leaves 16 h after spraying with $AgNO_3$

Gene	Locus	Down-regulation, fold
CYP706A6	At4g12320	2.0
CYP77A4	At5g04660	2.1
CYP86A8	At2g45970	2.1
CYP71B7	At1g13110	2.1
CYP705A4	At4g15380	2.1
CYP709A1	At5g38450	2.3
CYP707A2	At2g29090	2.5
CYP706A2	At4g22690	2.7
CYP705A3	At3g20960	2.7
CYP71A14	At5g24960	2.8
CAB43691	At4g32540	3.0
CYP707A3	At5g45340	3.0
CYP75B1	At5g07990	3.0
CAB94971	At3g55120	3.8
AAF23561	At5g13930	3.9

Four independent experiments were performed on an custom-designed oligoarray representing all *Arabidopsis* cytochromes P450 (CYP) and selected metabolic genes (see *Methods*).

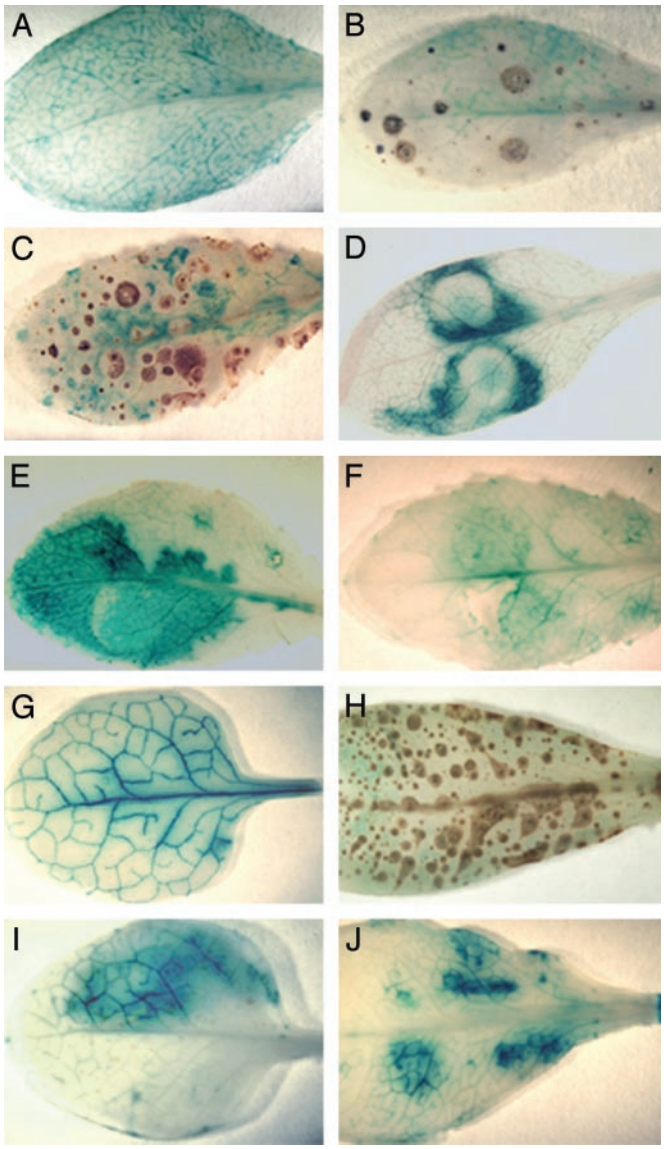

Fig. 3. GUS expression in rosette leaves of 6-week-old *CYP79B2p*::*GUS* and *CYP79B3p*::*GUS* plants after $AgNO_3$ and *P. syringae* treatment. *CYP79B2p*::*GUS* plants are shown untreated (*A*), 8 h after spraying with 5 mM $AgNO_3$ (*B*), 16 h after spraying with 5 mM $AgNO_3$ (*C*), 16 h after infiltration with *P. syringae* (*D*), 24 h after infiltration with *P. syringae* (*E*), and 24 h after infiltration with 10 mM $MgCl_2$ (control) (*F*). *CYP79B3p*::*GUS* plants are shown untreated (*G*), 16 h after spraying with 5 mM $AgNO_3$ (*H*), 24 h after infiltration with *P. syringae* (*I*), and 24 h after infiltration with 10 mM $MgCl_2$ (control) (*J*). Weakly colored rings (*D* and *E*) are syringe marks.

Discussion

In this article we demonstrate that camalexin is synthesized from IAOx that is derived from tryptophan in a reaction catalyzed by CYP79B2 and CYP79B3. In addition, we suggest that CYP79B2

and CYP79B3 have differential functions, because *CYP79B2* induction, specifically, is correlated with camalexin biosynthesis.

***In Vivo* Labeling of Camalexin.** We show that IAOx is a precursor for camalexin as evidenced by incorporation *in vivo* of externally applied fluorinated and ^{14}C-labeled IAOx into camalexin. Incorporation of radioactivity from [2′-^{14}C]IAOx shows that C-2′ in the thiazolin group of camalexin is derived from IAOx, which excludes incorporation of radioactivity via degradation of IAOx to free indole. In parallel experiments, we confirm that indole is a precursor (10). Fluorinated and ^{14}C-labeled tryptophan was incorporated with low efficiency. Low tryptophan incorporation has been observed in a study using ^{3}H-labeled tryptophan and anthranilate (8, 9) and led to the suggestion that tryptophan was not a direct, or was at best a poor, precursor of camalexin. Generally, interpretation of *in vivo* labeling experiments is complicated by difference in the ability of compounds to be taken up and transported to the site of the biosynthetic machinery that might be localized to different compartments even for the same pathway. In support of tryptophan-independency in camalexin biosynthesis, it was mentioned that the tryptophan synthase mutants *trp3–1* and *trp2–1* are not impaired in camalexin biosynthesis (8). However, it was recently shown that *trp3–1* is not tryptophan-limited, because it synthesizes elevated levels of tryptophan-derived glucobrassicin (28). Possibly, externally applied tryptophan is not efficiently transported to the compartment where camalexin is synthesized and/or it is consumed by other metabolic processes.

IAOx Is a Central Metabolic Branching Point in *Arabidopsis*. The absence of indole glucosinolates and camalexin in *Arabidopsis cyp79B2/cyp79B3* double mutant shows that only CYP79B2 and CYP79B3 contribute significantly to the IAOx pool(s), from which camalexin and indole glucosinolates are synthesized. Accordingly, neither the biochemically characterized plasma membrane-bound peroxidase catalyzing IAOx production (29) nor the proposed IAOx-forming pathway via YUCCA (30) contribute significantly to biosynthesis of camalexin or indole glucosinolates.

It has been hypothesized that cruciferous indole phytoalexins are derived from indole glucosinolates (5). However, we observe induction of camalexin in the mutant *sur1* that is completely blocked in its biosynthesis of glucosinolates (17). This finding excludes the possibility that camalexin is synthesized via indole glucosinolates. Interestingly, *in vivo* labeling of brassinin from *Brassica rapa* has shown more efficient incorporation of deuterated IAOx than deuterated indole glucosinolate into brassinin, suggesting that brassinin is not derived from the intact glucosinolate but directly from IAOx (19). Based on these observations and our data, we propose that all cruciferous indole phytoalexins with N- and S-containing side chains at the C-3 position are synthesized from tryptophan via IAOx in a reaction catalyzed by CYP79B homologs and that at least some of the indole phytoalexins including camalexin are not derived from indole glucosinolates.

Early enzymatic studies have identified IAOx as a precursor of IAA (16). A possible role of IAOx in IAA biosynthesis is further evidenced by the high-auxin phenotype of *sur1* and *sur2* that are blocked in postoxime enzymes in the glucosinolate pathway, resulting in channeling of IAOx into IAA (14, 17, 18). Expression of the IAOx-metabolizing CYP83B1 in glucosinolate biosynthesis was not significantly affected by treatment with $AgNO_3$ in our microarray experiments (Tables 1 and 2). Because CYP83B1 has a very high affinity for IAOx (14), this observation suggests that the IAOx-metabolizing enzymes in camalexin and IAA biosynthesis compete with CYP83B1 for IAOx, unless independent pools exist. Interestingly, *S*-alkyl thiohydroximate intermediates that are produced *in vitro* by the oxime-metabolizing CYP83 enzymes in the glucosinolate pathway undergo internal cyclization to form a thiazoline ring with structural similarity to the thiazol ring in camalexin (15). CYP83A1 and CYP83B1 belong phylogenetically to the CYP71 family (31), as does the oxime-metabolizing enzyme in the biosynthesis of cyanogenic glucosides (32). This relationship suggests that the oxime-metabolizing enzyme in camalexin biosynthesis may belong to the CYP71 family. CYP71B15/PAD3 is implicated to be involved in camalexin biosynthesis.

In conclusion, IAOx represents an interesting metabolic branching point, at which the flux of IAOx into camalexin, indole glucosinolates, and IAA must be controlled in a well structured organization at the 3D level of the different metabolons.

Differential Function of CYP79B2 and CYP79B3 in Camalexin Biosynthesis. A difference in the expression pattern of *CYP79B2* and *CYP79B3* was observed in rosette leaves 16 h after $AgN0_3$ treatment. The transcript level of *CYP79B2*, and not that of *CYP79B3*, was increased, as is evident from our cytochrome P450 microarray data. Similarly, GUS staining of leaves after $AgNO_3$ treatment showed induction of *CYP79B2,* but not of *CYP79B3*, and the induction was localized to areas surrounding spots that received $AgNO_3$ spray (Fig. 3*C*). This finding suggests that the local induction of *CYP79B2* in the leaf is much higher than observed in the array data where whole-leaf RNA was used. The GUS and array data are in agreement with the observed tendency to reduction of camalexin production in the *cyp79B2* mutant compared with the *cyp79B3* mutant (Fig. 2).

The effect of infection with camalexin-inducing pathogens on gene expression has been investigated in a number of microarray technology studies. We surveyed the available array data to evaluate our observation that CYP79B2 and CYP79B3 play different roles in camalexin biosynthesis. Upon *Alternaria brassicola* infection, *CYP79B2* was induced 3-fold after 24 h and 4.7-fold after 48 h induction (33). By using the same pathogen in a different experimental setup, as high as 45-, 50-, and 71-fold induction of CYP79B2 was observed in WT plants 12, 24, and 36 h, respectively, after infection (34). Upon *P. syringae* pv. ES4326 infection, a 27- to 42-fold induction of *CYP79B2* was observed after 30 h (35), in accordance with our GUS-staining data after infection with *P. syringae* DC3000/*avrRps4*. Under the various experimental conditions, no or minor *CYP79B3* induction was detected. The strong induction of *CYP79B2* by eukaryotic and prokaryotic pathogens and by the abiotic elicitor $AgNO_3$ indicates that *CYP79B2* plays a critical role in camalexin biosynthesis.

In *CYP79B2* overexpressing plants, no elevated camalexin levels have been observed. Therefore, the rate-limiting step of camalexin biosynthesis after $AgNO_3$ induction is downstream of IAOx. The transcript level of *CYP71B15/PAD3* was shown to be strongly induced by both *A. brassicola* and *P. syringae* infection (34, 35) but not significantly increased 16 h after $AgNO_3$ treatment in our microarray experiment, despite camalexin induction. A possible explanation is that *CYP71B15/PAD3* induction is stronger after treatment with *A. brassicola* and *P. syringae* in comparison with $AgNO_3$, and the constitutive *CYP71B15/PAD3* level is sufficient for camalexin response, suggesting a yet unknown enzyme to be rate-limiting for camalexin biosynthesis.

In summary, the present data have made us reformulate the biosynthetic pathway of camalexin, because we demonstrate that camalexin is synthesized from tryptophan via IAOx by CYP79B homologues and that it is not derived from glucosinolates or their degradation products. This is an important step in the elucidation of the biosynthetic pathways of cruciferous indole phytoalexins for future metabolic engineering of plants with improved disease-resistance and cancer-prevention properties. The data show that IAOx is a key branching point between several

secondary metabolic pathways as well as primary metabolism, where IAOx has been shown to play a critical role in IAA homeostasis.

We thank Dr. Catherine Bellini for providing *sur1* seeds, Dr. Yunde Zhao for providing seeds of *cyp79B2*, *cyp79B3*, and *cyp79B2/cyp79B3* mutants, originated from the SALK collection (Salk Institute Genomic Analysis Laboratory), Prof. Alfons Gierl for his continuous support, Charlotte Kristensen, Marc Morant, Dr. Mari-Anne Newman, and Dr. Bent Larsen Petersen for helpful suggestions, Katharina Lange and Thomas Rauhut for practical help, and Dr. Søren Bak for providing the P450 array. Funding for the SIGnAL-indexed insertion mutant collection was provided by the National Science Foundation. This work was supported by a European Molecular Biology Organization long-term fellowship (to E.G.) and Deutsche Forschungsgemeinschaft Grant GL346/1.

1. Pedras, M. S. C., Okanga, F. I., Zaharia, I. L. & Khan, A. Q. (2000) *Phytochemistry* **53,** 161–176.
2. Glawischnig, E., Mikkelsen, M. D. & Halkier, B. A. (2003) in *Sulphur in Plants*, eds. Abrol, Y. & Ahmad, A. (Kluwer, Dordrecht, The Netherlands), pp. 145–162.
3. Mezencev, R., Mojzis, J., Pilatova, M. & Kutschy, P. (2003) *Neoplasma (Bratisl.)* **50,** 239–245.
4. Zhang, Y., Talalay, P., Cho, C.-G. & Posner, G. H. (1992) *Proc. Natl. Acad. Sci. USA* **89,** 2399–2403.
5. Hanley, A. B., Parsley, K. R., Lewis, J. A. & Fenwick, G. R. (1990) *J. Chem. Soc. Perkin Trans. 1*, 2273–2276.
6. Tsuji, J., Jackson, E. P., Gage, D. A., Hammerschmidt, R. & Somerville, S. C. (1992) *Plant Physiol.* **98,** 1304–1309.
7. Thomma, B. P., Nelissen, I., Eggermont, K. & Broekaert, W. F. (1999) *Plant J.* **19,** 163–171.
8. Tsuji, J., Zook, M., Hammerschmidt, R., Somerville, S. & Last, R. (1993) *Physiol. Mol. Plant Pathol.* **43,** 221–229.
9. Zook, M. & Hammerschmidt, R. (1997) *Plant Physiol.* **113,** 463–468.
10. Zook, M. (1998) *Plant Physiol.* **118,** 1389–1393.
11. Frey, M., Chomet, P., Glawischnig, E., Stettner, C., Grün, S., Winklmair, A., Eisenreich, W., Bacher, A., Meeley, R. B., Briggs, S. P., *et al.* (1997) *Science* **277,** 696–699.
12. Hull, A. K., Vij, R. & Celenza, J. L. (2000) *Proc. Natl. Acad. Sci. USA* **97,** 2379–2384.
13. Mikkelsen, M. D., Hansen, C. H., Wittstock, U. & Halkier, B. A. (2000) *J. Biol. Chem.* **275,** 33712–33717.
14. Bak, S., Tax, F. E., Feldmann, K. A., Galbraith, D. W. & Feyereisen, R. (2001) *Plant Cell* **13,** 101–111.
15. Hansen, C. H., Du, L., Naur, P., Olsen, C. E., Axelsen, K. B., Hick, A. J., Pickett, J. A. & Halkier, B. A. (2001) *J. Biol. Chem.* **276,** 24790–24796.
16. Helminger, J., Rausch, T. & Hilgenberg, W. (1985) *Phytochemistry* **24,** 2497–2502.
17. Mikkelsen, M. D., Naur, P. & Halkier, B. A. (2004) *Plant J.* **37,** 770–777.
18. Barlier, I., Kowalczyk, M., Marchant, A., Ljung, K., Bhalerao, R., Bennett, M., Sandberg, G. & Bellini, C. (2000) *Proc. Natl. Acad. Sci. USA* **97,** 14819–14824.
19. Pedras, M. S. C., Montaut, S., Xu, Y., Khan, A. Q. & Loukaci, A. (2001) *Chem. Commun.*, 1572–1573.
20. Zhao, Y., Hull, A. K., Gupta, N. R., Goss, K. A., Alonso, J., Ecker, J. R., Normanly, J., Chory, J. & Celenza, J. L. (2002) *Genes Dev.* **16,** 3100–3112.
21. Hofmann, F., Rausch, T. & Hilgenberg, W. (1981) *J. Labelled Compds. Radiopharm.* **18,** 1491–1495.
22. Kane, M. D., Jatkoe, T. A., Stumpf, C. R., Lu, J., Thomas, J. D. & Madore, S. J. (2000) *Nucleic Acids Res.* **28,** 4552–4557.
23. Tusher, V. G., Tibshirani, R. & Chu, G. (2001) *Proc. Natl. Acad. Sci. USA* **98,** 5116–5121.
24. Glazebrook, J. & Ausubel, F. M. (1994) *Proc. Natl. Acad. Sci. USA* **91,** 8955–8959.
25. Hinsch, M. & Staskawicz, B. (1996) *Mol. Plant–Microbe Interact.* **9,** 55–61.
26. Zhou, N., Tootle, T. L. & Glazebrook, J. (1999) *Plant Cell* **11,** 2419–2428.
27. Mert-Türk, F., Bennet, M. H., Mansfield, J. H. & Holub, E. B. (2003) *Physiol. Mol. Plant Pathol.* **62,** 137–145.
28. Müller, A. & Weiler, E. W. (2000) *Planta* **211,** 855–863.
29. Ludwig-Müller, J. & Hillgenberg, W. (1992) *Plant Cell Physiol.* **38,** 1115–1125.
30. Zhao, Y., Christensen, S. K., Fankhauser, C., Cashman, J. R., Cohen, J. D., Weigel, D. & Chory, J. (2001) *Science* **291,** 306–309.
31. Paquette, S. M., Bak, S. & Feyereisen, R. (2000) *DNA Cell Biol.* **19,** 307–317.
32. Bak, S., Kahn, R. A., Møller, B. L. & Halkier, B. A. (1998) *Plant Mol. Biol.* **36,** 393–405.
33. Narusaka, Y., Narusaka, M., Seki, M., Ishida, J., Nakashima, M., Kamiya, A., Enju, A., Sakurai, T., Satoh, M., Kobayashi, M., *et al.* (2003) *Plant Cell Physiol.* **44,** 377–387.
34. Van Wees, S. C., Chang, H. S., Zhu, T. & Glazebrook, J. (2003) *Plant Physiol.* **132,** 606–617.
35. Glazebrook, J., Chen, W., Estes, B., Chang, H. S., Nawrath, C., Metraux, J. P., Zhu, T. & Katagiri, F. (2003) *Plant J.* **34,** 217–228.